recycling

MDPI

Article

A Two-Layer Multi-Criteria Framework for Waste Foundry-Sand Concrete: Weighting Robustness, Streamlined Carbon Accounting, and Cross-Compilation Consistency

Ferdinand Niyonyungu and Aurobindo Ogra *

Department of Urban and Regional Planning, Faculty of Engineering and the Built Environment, University of Johannesburg, Doornfontein, Johannesburg 2094, Gauteng, South Africa; fniyonyungu@gmail.com
* Correspondence: aogra@uj.ac.za

Abstract

Waste foundry sand (WFS) can replace fine aggregate in concrete, but mix evaluations often rely solely on compressive strength or use multi-criteria models prone to double-counting. This research presents a two-layer decision framework applied to a published database of 233 mixes from 40 studies; a source audit of every original paper retained 196 mixes from 33 studies. Layer 1 evaluates fine-aggregate substitution using a three-criterion index (composite mechanics, mass-basis sand-displacement carbon savings, and material cost differential; variance inflation factors 1.0 to 1.5). Layer 2 isolates cement-inclusive global-warming potential (GWP), which is collinear with material cost inside a weighted index (VIF about 24). A mixed-effects model shows a 28-day strength equivalent to the control within ±1.8 MPa up to 30% replacement (−0.5 MPa, 95% CI −2.0 to 1.0), but the effect varies widely between foundry sands. Rankings agree across five weighting and aggregation schemes (Spearman $\rho \geq 0.84$), while haul-distance uncertainty limits the robust short-list to 13 mixes. The carbon saving is at most 5.1 kg CO_2e/m^3 and is lost if WFS processing emits more than about 8 kg CO_2e per ton at baseline haul distances. Under the baseline scenario, seven observed mixes are Pareto-efficient, none exceeding 355 kg/m^3 cement content. A secondary 112-record compilation, an estimated 61% of which probably overlaps the primary database, gives consistent results.

Keywords: waste foundry sand; sustainable concrete; multi-criteria decision analysis; streamlined carbon accounting; uncertainty analysis; Pareto efficiency; mixed-effects model; circular economy

Check for updates

Academic Editor: Sha Liang

Received: 19 October 2026
Revised: 16 November 2026
Accepted: 17 November 2026
Published: 22 November 2026

Copyright: © 2026 by the authors. Licensee MDPI, Basel, Switzerland. This article is an open access article distributed under the terms and conditions of the Creative Commons Attribution (CC BY) license.

1. Introduction

Each year, the global demand for sand and gravel reaches approximately 50 billion tons, driving widespread degradation of river systems and coastlines [1]. Aggregate contributes a small share of the cradle-to-gate greenhouse-gas emissions of concrete [2–4], but the scale of extraction and the parallel problem of industrial by-product disposal make aggregate substitution an important circular-economy strategy [5]. Waste foundry sand (WFS), a high-silica by-product of metal casting, is one such candidate. Approximately one ton of foundry sand is required for each ton of iron or steel castings [6], and in major industrial economies such as the United States, less than 30% of the spent foundry sand generated annually is estimated to be recycled [7].

While a substantial body of experimental research has evaluated WFS as a fine-aggregate replacement [8–13], complemented by recent studies applying machine-learning

algorithms to predict its mechanical properties [14–21], decision support systems are still less developed. Attempts to synthesize mechanical, environmental, and economic indices consistently run into three main structural flaws. Subjective weighting choices, such as those derived from the Analytic Hierarchy Process [22], frequently lack the sensitivity analyses needed to verify if conclusions stand under different weighting schemes [23]. Beyond weighting bias, composite frameworks routinely suffer from internal double-counting. Incorporating a standalone waste-utilization term alongside an embodied-carbon metric that scales linearly with replacement rate double-rewards material substitution, which conflicts with established guidelines on correlated indicators [24,25]. A further methodological oversight stems from misinterpreting model consistency as validation. Simply applying an index to a separate dataset demonstrates parallel performance rather than true validity. These shortcomings are exacerbated by the reliance on single-indicator carbon metrics that ignore broader ecological impacts [26], highlighting the need for multi-criteria frameworks that explicitly map criteria interactions [27].

To address these methodological gaps, this study establishes a two-layer assessment framework for WFS concrete using publicly available data. Specifically, this work introduces a composite mechanical index derived from three measured properties and verified against a principal-component alternative. It pairs a streamlined, producer-boundary carbon-accounting term for aggregate substitution, which is strictly distinct from a full life-cycle assessment, with a separate cement-inclusive specification layer, providing a quantitative demonstration of why these two scopes must remain decoupled. Furthermore, the framework integrates a material-cost proxy anchored to published price statistics alongside a rigorous comparison of subjective and objective weighting methods, distance-to-ideal aggregation, and collinearity diagnostics. Parameter uncertainty is explicitly propagated using literature-anchored distributions, mix-specific haul distances, and Sobol sensitivity indices. The study also performs non-dominated sorting of observed mixes while testing whether a continuous-optimization surrogate is statistically defensible, concluding with a cross-compilation consistency check on a secondary database that identifies and accounts for dataset overlap. Before any analysis, all 40 source papers of the primary database were checked against the database to confirm the replacement basis, specimen type, binder, and mix composition. Figure 1 summarizes the framework. The results are reported in Section 2, discussed in Section 3, and the data and methods are described in Section 4.

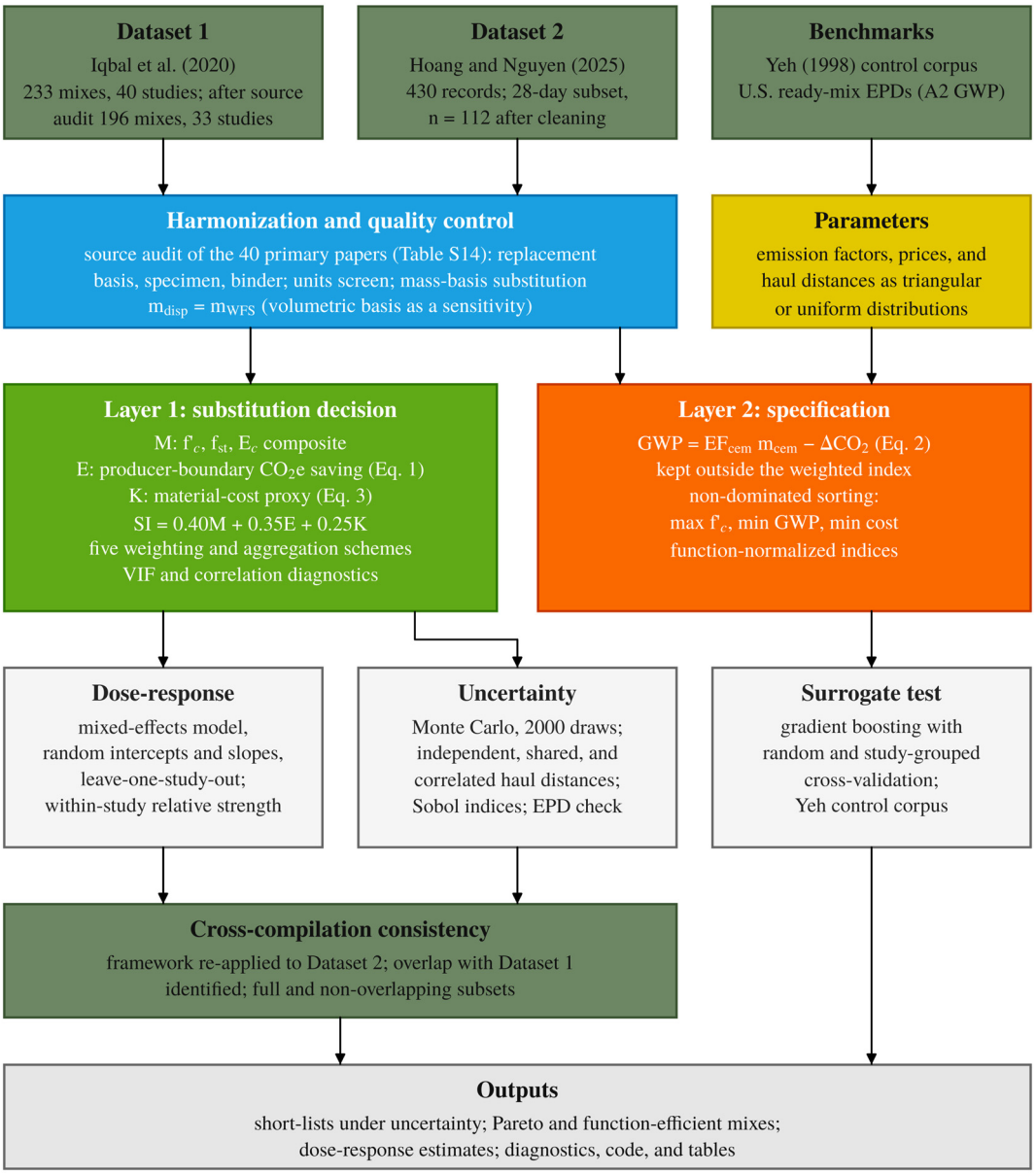


Figure 1. Workflow of the two-layer framework: datasets, source audit, harmonization and units screen, the substitution-decision layer, the cement-inclusive specification layer, supporting analyses, and outputs. Datasets from Iqbal et al. (2020) [14], Hoang and Nguyen (2025) [21], and Yeh (1998) [28].

2. Results

2.1. Criterion Redundancy

The three index criteria are not redundant, as evidenced by their Variance Inflation Factors (VIFs) of 1.03 (M), 1.50 (E), and 1.48 (K). The highest absolute Spearman correlation among these criteria is 0.49, between E and K (refer to Figure 2a and Table S2). The auxiliary indicators performed as anticipated. Circularity is aligned with E due to their mutual scaling with WFS use, while the cement-inclusive environmental variant aligns with K, as both scale with cement. Consequently, both indicators are excluded from the weighted index, because adding circularity raises the VIFs of E and circularity to 37.0 and 33.7, and substituting the cement-inclusive term for E raises the VIFs of that term and K to 24.1 and 24.3 (see Sections 2.4 and 4.7 and Figure 2b). Low VIFs show limited linear collinearity across the corpus, not independence; within a mix family, E and K are redundant (Section 2.3).

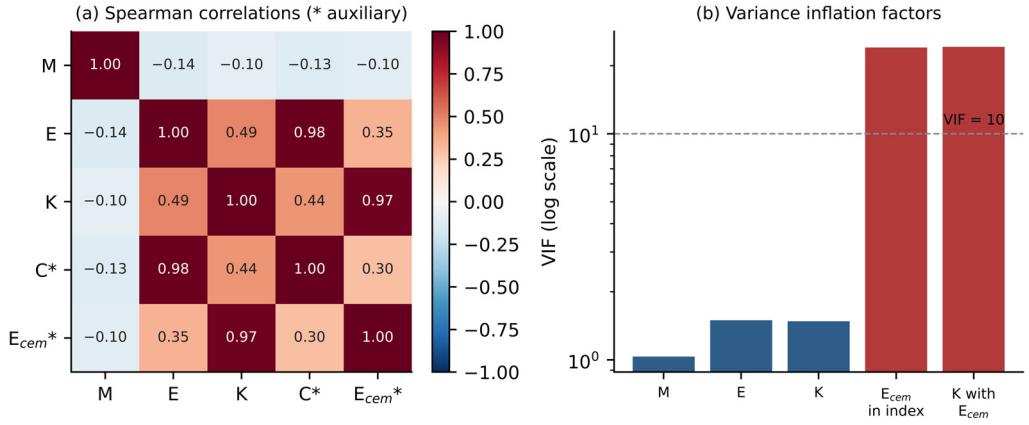


Figure 2. Redundancy diagnostics. (**a**) Spearman correlations among the index criteria (M, E, K) and auxiliary indicators marked with an asterisk (C, circularity; E_{cem}, cement-inclusive environmental term). (**b**) Variance inflation factors for the baseline index and for an index in which the cement-inclusive term replaces E.

2.2. Mechanical Dose-Response with Study Effects

In the mixed-effects model (refer to Table 1 and Figure 3a), the water-to-cement ratio (w/c) was the predominant fixed effect, exhibiting a decrease of 120.7 MPa per unit ($p = 9 \times 10^{-12}$). The cement coefficient was −5.5 MPa per 100 kg/m^3 ($p = 0.050$). After the source audit, the retained w/c range is narrow (0.40 to 0.56) and w/c and cement content are correlated ($\rho = -0.74$), so these two coefficients should not be interpreted separately. The linear term of the waste foundry sand (WFS) was not significant (+0.10 MPa per unit of x, $p = 0.77$), whereas the quadratic term was (−0.090 MPa per unit of x^2, $p = 0.020$); their combined effect therefore intensified with increased replacement. The estimated changes were −0.2 MPa at 20% replacement (95% CI: −1.3 to 1.0), −0.5 MPa at 30% (−2.0 to 1.0), −1.7 MPa at 50% (−3.6 to 0.2), and −8.0 MPa at 100% (−11.1 to −4.8). At a margin of ±1.8 MPa, the change is equivalent to zero up to 30% replacement (90% CI at 30%: −1.7 to 0.7) but not at 50% (Table S15g). The intraclass correlation coefficient was 0.68, indicating that approximately two-thirds of the residual variance, after accounting for covariates, was attributable to differences between studies. This suggests that pooled statistics may overestimate the precision of any WFS effect. Adjusting for the median w/c and cement content and excluding the study intercepts reduced the standard deviation of the plotted strengths from 7.4 to 4.0 MPa.

Table 1. Mixed-effects model for 28-day compressive strength (study random intercepts; $n = 178$ mixes, 30 studies after the source audit and units screen; intraclass correlation = 0.68).

Term	Coefficient	Standard Error	*p*
Intercept (MPa) [a]	114.9	17.6	6×10^{-11}
WFS, linear term (x)	+0.10	0.35	0.77
WFS, quadratic term (x^2)	−0.090	0.038	0.020
w/c (per unit) [b]	−120.7	17.7	9×10^{-12}
Cement (per 100 kg/m^3) [b]	−5.5	2.8	0.050

Fitted change in f'_c relative to 0% WFS = +0.10x − 0.090x^2; for example, −0.5 MPa at 30% replacement (x = 3). [a] The intercept is the model constant (predicted strength at w/c = 0 and zero cement) and has no physical meaning. [b] w/c and cement content are correlated in the retained data ($\rho = -0.74$; w/c 0.40 to 0.56), so their coefficients are not separately interpretable.

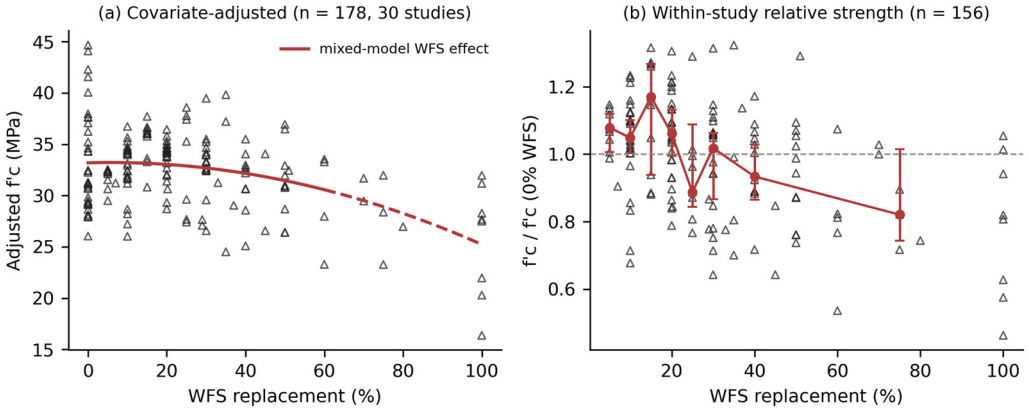


Figure 3. Dose-response of the 28-day compressive strength. (**a**) Covariate-adjusted strengths (adjusted to the median w/c and cement content, with study random intercepts removed) and the mixed-model WFS effect, dashed beyond 60% replacement where data are sparse. (**b**) Within-study relative strength against each series' own 0% WFS control, with band medians and cluster-bootstrap 95% intervals. Open triangles are individual mixes, and the dashed line in (**b**) marks a strength ratio of 1.0 (equal to the control).

The WFS effect is not the same in every study. Adding a random slope on x improved the fit (likelihood-ratio $p = 2 \times 10^{-6}$), with a between-study standard deviation of 1.6 MPa per 10 percentage points of replacement. The average effect barely changed (−0.6 MPa at 30%), but the 95% prediction interval for a new foundry sand at 30% replacement is −10.2 to +9.0 MPa. Leaving out each study in turn moved the average change between −0.8 and 0.0 MPa at 30% and between −2.2 and −1.1 MPa at 50% (Table S15f). The confidence interval for the average effect therefore does not predict how a particular foundry sand will perform; each new source has to be tested.

The relative strengths observed within the study (Figure 3b; 156 records, 33 studies) consistently indicate that up to a 20% replacement, the band medians are at or exceed unity. Specifically, for replacements between 5% and 10%, the median is 1.05 with a 95% confidence interval (CI) of 1.00 to 1.10, and for 15% to 20%, the median is 1.06 with a CI of 1.00 to 1.13. In the range of 20% to 50% replacement, the medians vary from 0.89 to 1.02, with confidence intervals encompassing unity (20% to 25%: 0.89, CI 0.84 to 1.09; 30% to 50%: 0.93, CI 0.87 to 1.03). For replacements exceeding 50%, the median decreases to 0.82, with a confidence interval of 0.74 to 1.01. Overall, WFS shows no detectable average loss of 28-day strength up to 50% replacement and equivalence within ±1.8 MPa up to 30%, consistent with experimental findings [9,29]; a clear loss appears only at high replacement (−8.0 MPa at 100%). The exclusion of the 28 records identified as outliers in the source database results in minimal changes to these estimates (−0.4 MPa at 30%; see Supplementary Table S5). Converting cube strengths to cylinder-equivalent values (−0.6 MPa at 30%) or adding specimen type as a covariate (cylinder term $p = 0.48$; −0.5 MPa at 30%) also leaves the estimate essentially unchanged.

2.3. Weighting and Aggregation Robustness

Among the five ranking methods, all pairwise Spearman correlations were at least 0.84, with top-quintile overlaps reaching a minimum of 69% (refer to Figure 4b and Table S3). Notably, the entropy scheme deviates by allocating 0.71 of the weight to the high-dispersion environmental criterion. The rankings derived from the equal, CRITIC, and CRITIC-TOPSIS methods align with the stakeholder scenario, exhibiting a correlation coefficient (ρ) of at least 0.98. Furthermore, the desirability index shows a correlation of $\rho = 0.78$ with the SI across all mixes and $\rho = 0.89$ across the 138 mixes that include WFS.

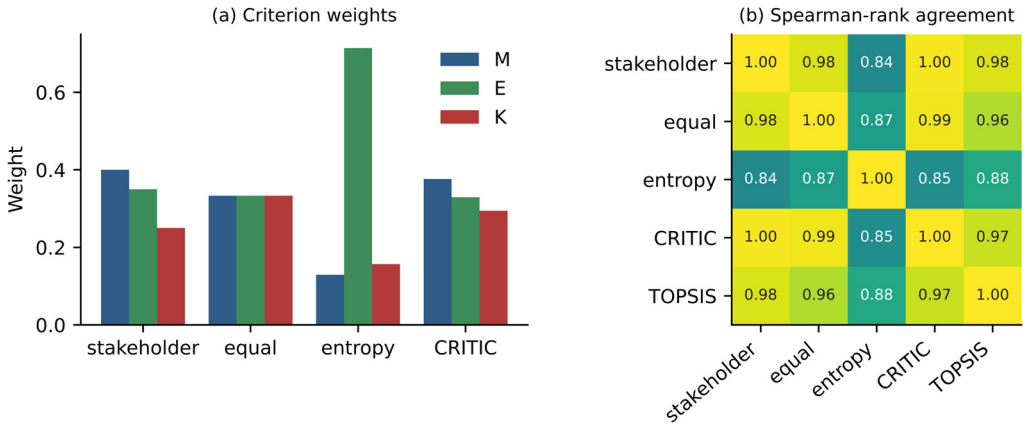


Figure 4. Weighting and aggregation. (**a**) Criterion weights by method. (**b**) Spearman-rank agreement among the stakeholder, equal, entropy, CRITIC, and CRITIC-TOPSIS rankings.

Under baseline weights, SI correlated with WFS replacement at $\rho = 0.66$. This association is built into the index mainly through a single criterion: E correlates with replacement at $\rho = 0.98$, whereas the mechanical and cost criteria combined correlate with it at $\rho = 0.18$. Across the corpus, the index therefore rewards substitution mainly through E. Its top quintile had a median replacement of 50%, and 57% of those mixes contained at least half WFS. When the mechanical eligibility screen is applied (126 retained mixes), the association falls to $\rho = 0.58$, and the median replacement in the top quintile falls to 30% (median relative strength 1.03). For users who cannot accept a strength penalty, the screened index is more appropriate.

Across the corpus, E and K are only moderately correlated ($\rho = 0.49$), because cement content dominates cost. Within a family of mixes with the same cement content and w/c, however, the substitution differential in K and the saving in E both scale with WFS mass, and they are perfectly rank-correlated ($\rho = 1.00$ in all 31 families with three or more mixes). Inside a family, substitution therefore enters the index with the combined weight of E and K (0.60 at baseline). Replacing K with the cement cost alone, which is constant within a family, removes this overlap; the rankings barely change ($\rho = 0.993$ with the baseline; top-quintile overlap 94%; VIF 1.03 to 1.17), and the SI-WFS association falls to 0.60 (Table S15k). The rankings are also insensitive to normalization (Table S15b: $\rho \geq 0.991$ and top-quintile overlap $\geq$ 94% for winsorized bounds, fixed reference bounds, and normalization pooled with Dataset 2) and to the mechanical criterion; with compressive strength alone, $\rho = 0.987$ with the baseline across all mixes and 0.990 within the 67 mixes that report all three properties (Table S15c). With cube strengths converted to cylinder-equivalent values, $\rho = 0.985$ with the baseline and the top-quintile overlap is 86% (per-mix values in Table S15k).

2.4. Why the Framework Has Two Layers

Two results justify separating the layers. First, if the cement-inclusive GWP replaces E inside the index, the VIFs of that term and of the cost criterion rise to 24.1 and 24.3, because both are nearly linear in cement content; the nominally three-dimensional decision space then collapses toward a single cement dimension (Figure 2b). Second, the two scopes answer different questions and rank mixes differently. The baseline index and its cement-inclusive variant correlate at $\rho = 0.80$ and share only 71% of their top quintiles (Figure 5), with high-cement mixes losing rank once their binder burden is counted. The practical rule is to use the index to decide whether and how much WFS to use within a mix family, and the specification layer to choose among competing designs, since the fine-aggregate

saving (at most 5.1 kg CO_2e/m^3) cannot compensate for binder differences (median cement burden about 328 kg CO_2e/m^3).

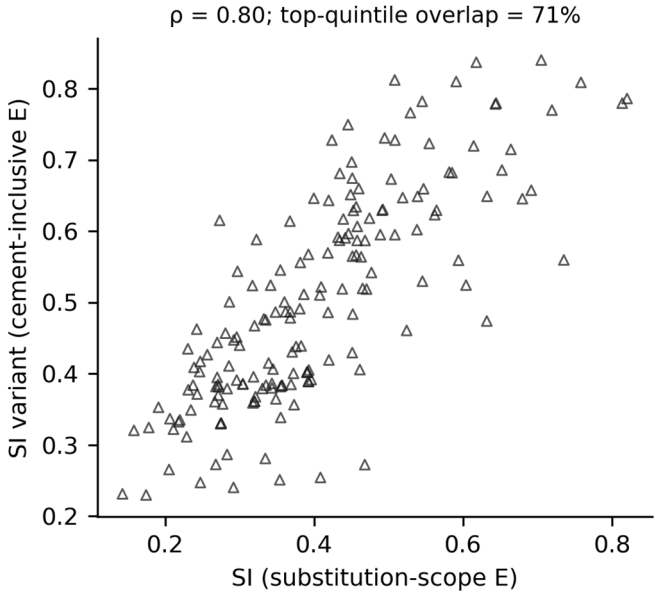


Figure 5. Baseline (substitution-scope) index versus its cement-inclusive variant.

2.5. Uncertainty and Global Sensitivity

Parameter uncertainty is large relative to the differences between many mixes. The median width of the 95% interval on SI is 0.15 (Figure 6a; Table S6), the median rank correlation between Monte Carlo draws and the baseline ranking is 0.85 (fifth percentile 0.79), and 34% of mixes change SI quartile in a typical draw (Figure 6b). Rankings should therefore be used as short-lists rather than as point orderings. Thirteen mixes from six studies are in the top quintile in at least 90% of draws. They have WFS replacements of 0% to 75%, cement contents of 320 to 400 kg/m^3, and strengths of 42.5 to 56 MPa, and four of them are controls without WFS. Most high-replacement mixes rank highly at baseline but drop out of the robust short-list (only one mix with more than 50% WFS remains), because their advantage rests on the environmental criterion, which is the most sensitive to logistics.

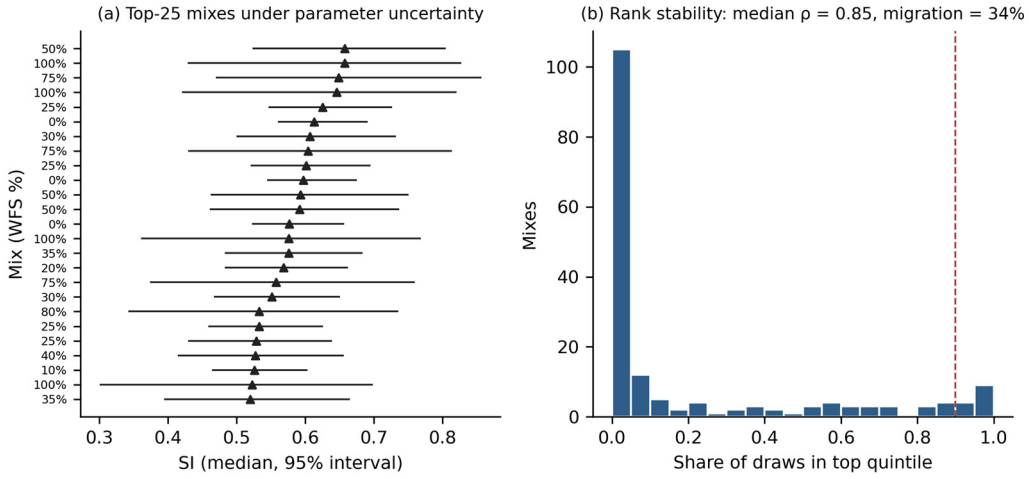


Figure 6. Uncertainty in substitution index. (**a**) Medians and 95% intervals for the 25 mixes with the highest median SI, labeled by WFS replacement. (**b**) Share of Monte Carlo draws in which each mix is in the top quintile; the dashed line marks the 90% threshold that defines the robust shortlist.

The short-list does not depend on assuming independent distances (Table S15d). When distances are shared by all mixes of a study, the median rank correlation is 0.86 and 12 mixes are short-listed, all of them on the baseline list; when the shared distances are also correlated between the two legs, it is 0.95 and 17 mixes are short-listed, 12 of them on the baseline list. With a single regional distance per draw, rankings are nearly unchanged in most draws (median $\rho = 0.999$) but invert when the WFS haul exceeds the sand haul (fifth percentile $\rho = 0.11$). Parameter uncertainty with distances fixed hardly moves the ranking (median $\rho = 0.9997$; quartile migration below 1%), whereas distance variability alone reproduces most of the baseline dispersion ($\rho = 0.88$; migration 31%); the rank instability is therefore a matter of between-site logistics rather than of the emission factors or prices. A volumetric run with the missing specific-gravity ratios drawn from the observed ones gives $\rho = 0.87$, and 13 of its 14 short-listed mixes are on the baseline list. Nine mixes from five studies, with 0% to 50% WFS, stay on the short-list under all four distance schemes.

The Sobol indices differ sharply between the two layers (Figure 7; Table S7). For the substitution term, the quarry-to-plant distance (S1 = 0.47, ST = 0.49) and the foundry-to-plant distance (S1 = 0.47, ST = 0.49) account for nearly all the variance, whereas the sand and freight-emission factors are minor; in 16% of samples, the representative mix has a net negative saving, which occurs when the WFS haul is long and the avoided sand haul is short. For cement-inclusive GWP, the cement emission factor accounts for essentially all the variance (S1 = 0.999). Both results follow from the relative magnitudes of the terms and are properties of the accounting rather than findings about materials. Their practical reading is that logistics determine whether the substitution saving materializes, whereas the binder determines the climate performance of the concrete.

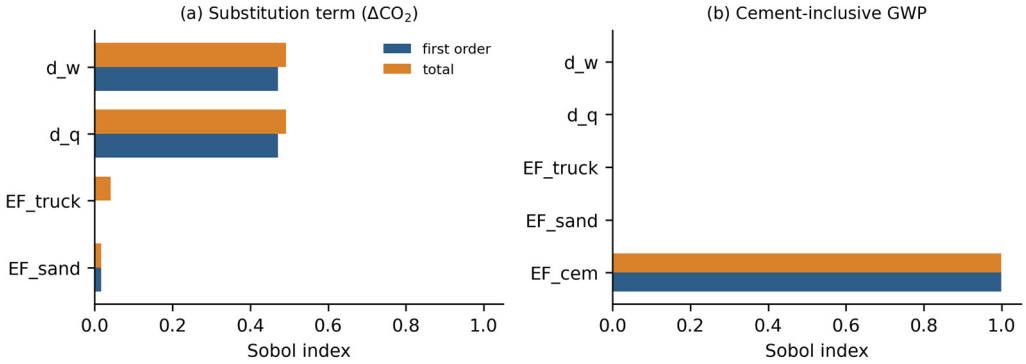


Figure 7. First-order and total Sobol indices for a representative mix (median WFS and cement content): (**a**) substitution-scope ΔCO_2; (**b**) cement-inclusive GWP.

The EPD benchmark places these distances in context (Figure 8a; Table S13). Across 38,944 U.S. ready-mix EPDs, the A2 (transport to plant) contribution has a median of 28 kg CO_2e/m^3 (interquartile range 18 to 64), or 9.1% of A1 to A3 (cradle-to-gate production). At the baseline freight factor and a constituent mass of 2.3 t/m^3, the median corresponds to a mass-weighted one-way haul of approximately 102 km across all constituents, including cement. The 10 to 100 km range assumed for the fine-aggregate legs corresponds to 2.8 to 27.6 kg CO_2e/m^3 if applied to the whole mix, which covers the lower half of the market distribution (49% of EPDs). This is an envelope check, not a measurement of aggregate-specific hauls. The median transport burden in U.S. declarations is more than five times the largest substitution saving in the dataset.

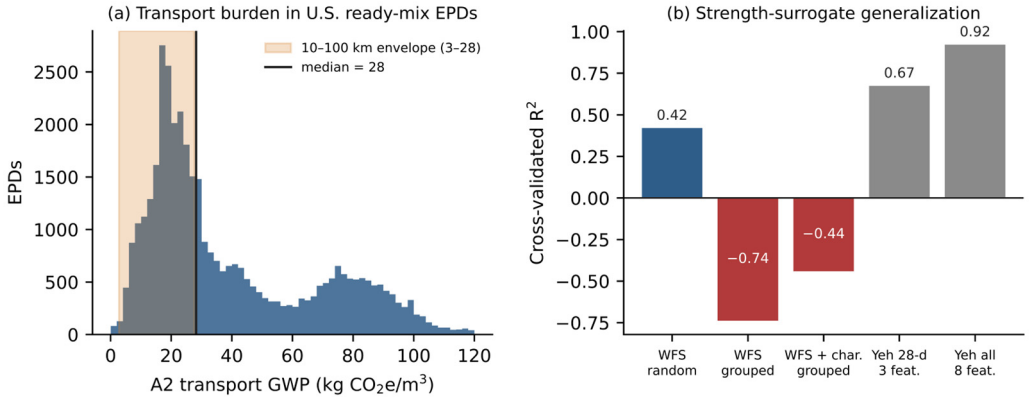


Figure 8. External benchmarks. (**a**) A2 transport GWP in 38,944 U.S. ready-mix EPDs [30] and the envelope implied by the assumed 10–100 km hauls. (**b**) Cross-validated R^2 of a gradient-boosting strength surrogate for the pooled WFS corpus (random and study-grouped folds, with and without WFS characterization) and Yeh database (random folds).

2.6. Multi-Objective Efficiency

The non-dominated sorting of the 173 indexed mixes in the specification space identified seven Pareto-efficient designs (4.0%; Figure 9). Their cement contents ranged from 300 to 355 kg/m^3; therefore, none of the 118 observed mixes with more cement was efficient under the baseline scenario. Binder-heavy designs that would rank well in terms of strength were dominated once their GWP and cost were considered. The WFS replacement in the efficient set ranged from 0% to 100%, and the strength ranged from 28.4 to 56.0 MPa, which shows that the replacement level by itself does not confer efficiency. Four of the seven mixes come from a single source study (study 16 in Table S14), so the set reflects a few laboratory programs.

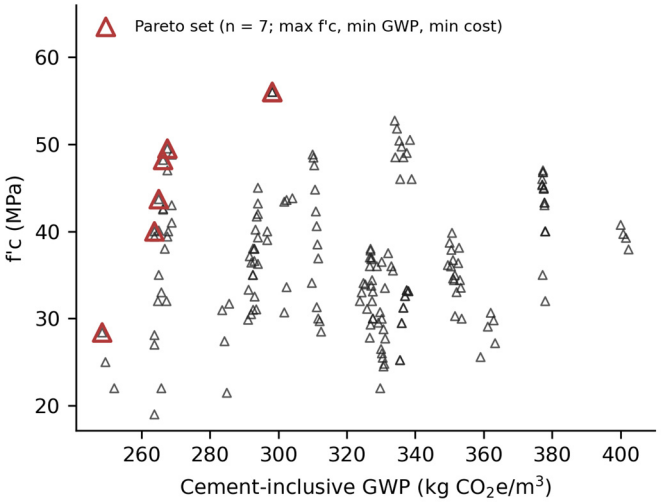


Figure 9. Observed mixes in the GWP-strength plane; open triangles mark the three-objective Pareto set (maximum f'_c, minimum GWP, minimum cost; per-mix values in Table S8).

Because GWP and cost are both governed by cement content, they are almost redundant as objectives ($\rho = 0.97$; f'_c correlates with GWP at 0.09 and with cost at 0.07), and sorting on strength and GWP alone gives the same seven mixes. The set is unchanged at $EF_{cem} = 0.58$ kg CO_2e/kg, at cement prices of USD 120 and 180/t, with water added at an upper-bound factor, and when mixes below 25 MPa are removed; with a 30 or 40 MPa minimum, it loses only the 28.4 MPa mix (Table S15e). Using substitution-scope carbon instead of GWP enlarges the set to 11 mixes, the cement-type factors to 12, and the cylinder-

equivalent strengths to 11; each contains all seven baseline mixes. In the Monte Carlo draws, four of the seven are efficient in at least 90% of draws. Non-dominance applies only within the observed mixes; it does not imply that no better design exists.

Function-normalized efficiency provides a different view (Figure 10; Table S9). In the column case, the (χ_{col}, κ_{col}) front contains four mixes with WFS replacements of 0%, 0%, 25%, and 50%, cement contents of 320 to 355 kg/m^3, and strengths of 48 to 56 MPa; all four are also in the per-cubic-meter Pareto set. In the cracking case, where strength enters only as $f'_c{}^{0.25}$, the front is four mixes from one study with 320 kg/m^3 of cement and 25%, 50%, 75%, and 100% WFS (40 to 50 MPa), which are also in the per-cubic-meter Pareto set; the two lower-replacement mixes are shared with the column front, so the preferred replacement level depends on the governing limit state. Eco-efficiency in the column case is driven by strength (Spearman ρ between χ_{col} and $f'_c = -0.86$); the strongest mixes, not those with the lowest GWP per cubic meter, are the most eco-efficient per unit of axial capacity, which echoes the finding of Tavares et al. [31] that per-volume carbon metrics are incomplete as standalone criteria. Pooled across studies, eco-efficiency shows no association with WFS content ($\rho = -0.09$; study-cluster 95% CI −0.28 to 0.14). Within studies, however, χ_{col} rises slightly with replacement ($\rho = 0.18$; within-study permutation $p = 0.03$), because strength tends to fall while GWP barely changes. In this corpus and for this simplified column formulation, WFS content was therefore not associated with improved structural eco-efficiency, and within studies the association was slightly unfavorable; these are associations, not causal estimates, and they apply at the cement contents and strengths observed. Because both numerators are cement-dominated and both share f'_c, χ_{col} and κ_{col} are almost collinear (Spearman $\rho = 0.99$); therefore, the column front is the efficient tail of a single ranking rather than a two-objective trade-off. These indices are member-level bounding cases (unreinforced-section simplifications) and complement the per-cubic-meter analysis.

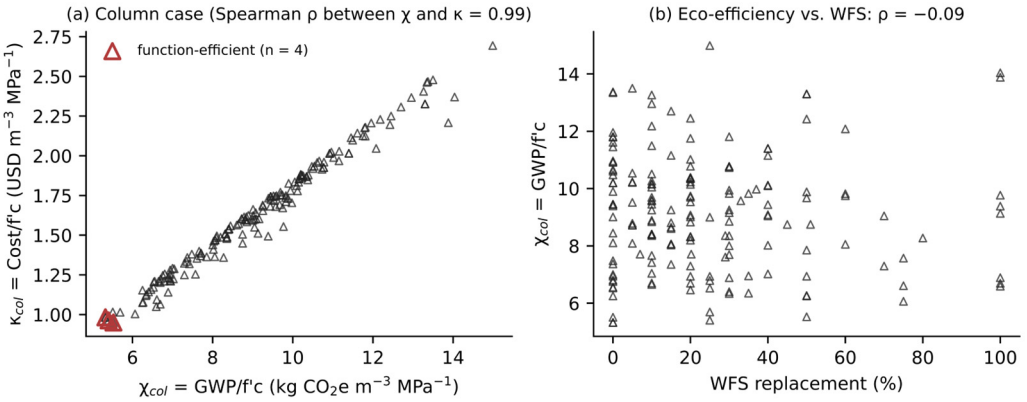


Figure 10. Function-normalized specification indices for the column case: (**a**) eco- versus cost-efficiency per unit axial capacity with the non-dominated set; (**b**) eco-efficiency versus WFS replacement. Open triangles are individual mixes.

Continuous optimization was not pursued because the strength surrogate did not generalize across studies (Figure 8b). With the mix descriptors alone, gradient boosting reached a mean R^2 of 0.42 under random five-fold cross-validation but −0.74 under study-grouped cross-validation; that is, it could not predict the strength of mixes from studies it had not seen. Adding the WFS characterization available in the database raised the grouped R^2 only to −0.44 (random: 0.59). For the single-program Yeh data, the same model class reached 0.67 with three descriptors (28-day subset, $n = 425$) and 0.92 with all inputs ($n = 1030$) under random cross-validation. The comparison of random with grouped folds on the WFS corpus is the like-for-like contrast: the drop from 0.42 to −0.74 measures between-study heterogeneity that the reported variables do not capture. Foundry sands differ in clay content, organic matter,

and binder chemistry (green versus chemically bonded sands), and these properties are rarely reported. Any optimum derived from a pooled surrogate would therefore be unreliable, and specification guidance is drawn only from observed non-dominated mixes.

2.7. Replacement Bands with Cluster-Aware Inference

Median SI rises across replacement bands, from 0.27 (0% to 5%) to 0.60 (50% to 100%), with cluster-bootstrap 95% intervals in Supplementary Table S10; the rise is not monotonic in the mid-range (15% to 20%: 0.38; 20% to 25%: 0.36; 25% to 30%: 0.51; 30% to 50%: 0.45). The Kruskal–Wallis test across bands gives $p = 2 \times 10^{-14}$ on individual records and $p = 3 \times 10^{-6}$ on 122 study-level band medians. Because band medians from the same study remain dependent, a mixed model with study random intercepts was also fitted (likelihood-ratio $p = 7 \times 10^{-34}$), and within studies SI rises with replacement ($\rho = 0.85$; within-study permutation $p = 0.0005$). All three tests agree, so the rise is not an artifact of repeated studies. Because the rise reflects the environmental criterion (Section 2.3), the band analysis should be read together with the dose-response: replacement up to about 30% delivers the substitution benefit at a 28-day strength equivalent to the control, whereas higher replacement trades strength for a small and logistics-dependent carbon saving.

2.8. Cross-Compilation Consistency

Applied unchanged to the second dataset, the framework gives results consistent with the primary dataset (refer to Tables 2 and S11; Figure 11). The association between SI and WFS is $\rho = 0.66$ in the primary dataset (also 0.66 when the primary index uses compressive strength alone, as the second dataset must), 0.73 in the complete second dataset (95% interval 0.54 to 0.81, from resampling mix series; Table S15h), and 0.68 in its 44 non-overlapping records (0.42 to 0.86). The rank agreement among the five methods remains high, with a minimum ρ of 0.90 in both the full dataset and the non-overlapping subset. The criteria show limited collinearity, with VIF values of 1.05 to 1.10 in the full dataset and 1.03 to 1.11 in the non-overlapping subset. Entropy weights vary between compilations, with a weight on E of 0.71 in the primary dataset, 0.58 (0.44 to 0.69) in the second, and 0.44 (0.28 to 0.60) in its non-overlapping subset. This variation is anticipated for a dispersion-based method, underscoring the necessity of reporting multiple schemes. The median strength by band exhibits minimal change across replacement bands in both compilations (see Figure 11b); these medians are not adjusted for water-to-cement ratio or cement content, and thus they do not contradict the covariate-adjusted loss at high replacement levels discussed in Section 2.2. Excluding the 24 records containing silica fume or fly ash reduces the SI-WFS association in the second dataset from 0.73 to 0.64 ($n = 88$; VIF 1.05 to 1.08; minimum rank agreement 0.84), and pricing their silica fume and fly ash at the cement price leaves it at 0.73. In the 20 non-overlapping records devoid of these materials, which are the cleanest test (eight series), the association is 0.41 (0.20 to 0.81), indicating limited evidence from the non-overlapping data. Given that 68 of the 112 cleaned records probably overlap with the primary dataset, the agreement in the full set partially reflects shared source data; the non-overlapping subset is small (17 series), and its intervals are wide, so it supports only qualitative conclusions, and the agreement between compilations is a consistency check, not independent replication.

Table 2. Key results for the primary dataset, the full and non-overlapping second dataset.

Metric	Dataset 1	Dataset 2 (Full)	Dataset 2 (Non-Overlap)
Records (series)	173	112 (30)	44 (17)
Spearman ρ, SI vs. WFS %	0.66	0.73 (0.54–0.81)	0.68 (0.42–0.86)

Table 2. *Cont.*

Metric	Dataset 1	Dataset 2 (Full)	Dataset 2 (Non-Overlap)
Minimum rank agreement, five methods	0.84	0.90	0.90
Entropy weight on E	0.71	0.58 (0.44–0.69)	0.44 (0.28–0.60)
VIF range (M, E, K)	1.03–1.50	1.05–1.10	1.03–1.11

Note: Non-overlap: series of Dataset 2 with no matching Dataset 1 on cement content, w/c, and WFS replacement. Values in parentheses are 95% intervals from resampling mix series.

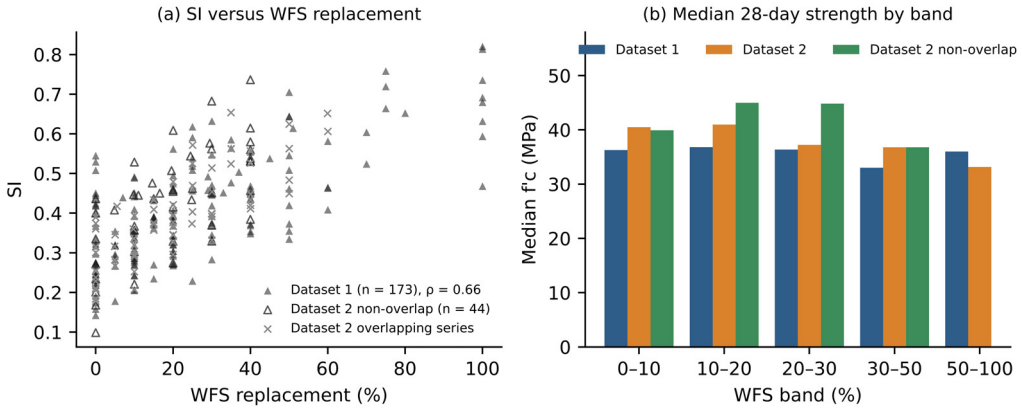


Figure 11. Cross-compilation consistency. (**a**) SI versus WFS replacement in the primary dataset and non-overlapping and overlapping parts of the second dataset. (**b**) Median 28-day strength by band replacement.

2.9. Foundry-Side Scenario and WFS Processing

Incorporating the avoided landfill haul and tipping fee increases the maximum carbon savings from 5.1 to 8.9 kg CO_2e/m^3 and reduces material costs by up to USD 39.7/m^3 for the highest waste foundry-sand (WFS) contents. Although rankings exhibit minor changes ($\rho = 0.97$ with the baseline; 91% top-quintile overlap), the association between substitution index (SI) and WFS rises to 0.75. This increase is attributed to the tipping-fee credit, which causes costs to decrease with WFS mass ($\rho = -0.85$). The allocation of these credits to the concrete producer is contingent upon the contractual agreements between the foundry and the producer; thus, they are presented as a scenario rather than a baseline.

Processing works in the other direction. At baseline haul distances, the saving is 7.9 kg CO_2e per ton of WFS; a beneficiation step that emits more than this cancels it. Over the distance distributions, the break-even burden has a median of 5.8 kg CO_2e/t and is negative in 16% of cases, where the WFS haul alone outweighs the avoided sand. The estimated thermal-drying burden exceeds this baseline break-even, at 8.4 to 11.2 kg CO_2/t at 2% moisture, 13.9 to 18.6 kg CO_2/t at 5%, and 19.4 to 25.9 kg CO_2/t at 8% (dryer efficiency 0.8 to 0.6; Table S15i), although at 2% moisture the margin is small and the 95th percentile of the break-even over the distance distributions is 15.2 kg CO_2e/t. Some source studies washed and sun-dried the sand before use [29]; air drying adds little emission, whereas kiln drying, at these estimated burdens and baseline distances, would cancel the saving. The substitution credit is therefore most defensible for WFS that can be used as received or air-dried; where WFS must be kiln-dried, its climate case rests on avoided landfill use alone. Under a uniform processing burden, the rankings are unchanged up to 6 kg CO_2e/t, and at 8 kg CO_2e/t or more no mix retains a net saving (Table S15j).

3. Discussion

3.1. Per-Volume Versus Per-Function Metrics

The function-normalized results substantiate the argument that using per-cubic-meter Global-Warming Potential (GWP) as a criterion in current procurement thresholds is insufficient, as it fails to account for variations in element volume due to strength changes [31–33]. Within this corpus, both function-normalized fronts are situated within the per-cubic-meter Pareto set; however, they select distinct mixes (strong mixes with 0% to 50% WFS for columns, and higher-replacement mixes of one study at the same cement content for cracking). In this corpus, WFS content was not associated with improved function-normalized eco-efficiency, and within studies the association was slightly unfavorable in the column case; these are associations under simplified member formulations, not causal effects. Consequently, frameworks and procurement rules should specify the question they address, whether it is the impact per cubic meter supplied or the impact per unit of structural function.

3.2. Comparison with Other Secondary Materials

Unlike supplementary cementitious materials, such as fly ash and ground granulated blast-furnace slag, which displace clinker and act on the dominant term of the carbon budget [3,32], WFS only acts on the small aggregate term. Its climate case rests on avoided extraction, avoided disposal, and logistics, not on binder decarbonization, and the Sobol results show that even this small saving depends on haul distances; Section 2.9 shows that, at baseline haul distances, the estimated burden of kiln drying would exceed it. WFS substitution and SCM substitution are therefore complementary levers. Foundry-specific concerns, such as leachability and organics in chemically bonded sands [34], are not captured by this framework.

3.3. What the Framework Does Differently

Composite indices for concrete tend to fail at three points: unexamined weights, double-counted substitution indicators, and dataset-relative normalization presented as absolute. The present framework does not remove subjectivity, which no multi-criteria method can do [25], but it bounds its consequences. Four weighting schemes and one distance-to-ideal aggregation agree at $\rho \geq 0.84$. Double counting across the corpus is checked (VIF 1.03 to 1.50), and the excluded circularity and cement-inclusive terms are reported with the collinearity evidence that excluded them (VIF about 37 and 24). Within a mix family, E and K carry the same substitution signal; a variant with cement-only cost removes this overlap without changing the rankings. The index still rewards substitution through E, and a mechanically screened variant is provided.

3.4. Limitations

Several important constraints shape the scope of these findings. Durability parameters remain entirely absent because chloride ingress, carbonation, freeze–thaw resistance, and shrinkage data are far too sparse in the existing literature to support an index term. Mixes that achieve high rankings here might therefore underperform in aggressive exposure settings, especially where residual clay or organic binders alter the long-term microstructure. As more comprehensive data emerge, researchers should treat durability metrics as eligibility constraints applied as preliminary pass or fail filters before ranking, rather than folding them into weighted criteria.

The scope is further restricted by the environmental metric addressing only climate impact, leaving leaching and other categories dependent on primary data collection. The economic evaluation relies on a simplified screening proxy that accounts solely for cement and the substitution differential instead of capturing total mix costs. Furthermore, be-

cause min–max normalization depends entirely on the specific corpus, the resulting index functions strictly as a relative ranking tool rather than an absolute score.

Data constraints also extend to physical and statistical properties. The baseline uses the mass basis reported by the source studies, so specific gravities enter only the volumetric sensitivity, in which 55 WFS-bearing mixes lacked them. Strength was measured on cubes in most source studies and on cylinders in a few (Table S14); converting cubes to cylinder-equivalent values changed the results little, but the conversion factor is generic. The WFS effect on strength varies between studies, so the average effects reported here do not replace testing of a new foundry sand. Literature compilations fail to capture batch-to-batch variability as well, which prevents any direct derivation of reliability-based design factors. Finally, because the two source compilations probably overlap substantially and feature a very small non-overlapping subset, observing cross-compilation agreement offers much weaker evidence than true independent replication would provide.

4. Materials and Methods

4.1. Primary Dataset

The primary dataset is the experimental database published as Supplementary Material by Iqbal et al. [14], which compiles 233 WFS concrete mixes with reported 28-day compressive strengths from 40 source studies. The variables included the water-cement ratio (w/c), WFS replacement of fine aggregate (%), WFS and cement contents (kg/m^3), properties of WFS and natural sand (fineness modulus, specific gravity, and absorption), compressive strength f'_c (MPa), split tensile strength (MPa, $n = 144$), and modulus of elasticity (GPa, $n = 79$). The study identity was retained for every record because records within a study share materials, laboratory practices, and curing conditions (Section 2.2). Entries carrying reporting symbols were cleaned, non-numeric values were treated as missing, and analyses were performed on an available-case basis with sample sizes reported throughout (cleaned data in Table S1). Of the retained records, the source database marked 28 records from 14 studies with an asterisk as outliers for at least one property; these records were kept in the main analysis, and their exclusion was tested in the Supplementary Materials (Tables S5 and S12).

All 40 source papers were obtained and checked against the database (Table S14). For each study, the replacement basis, the specimen used for compressive strength, the cement type, and the composition of the mixes taken into the database were recorded. Seven studies (37 records) were excluded because the effect of WFS could not be isolated or the binder was not Portland cement. In four of them, every WFS mix also contained bottom ash or fly ash that the control mix did not, and in two of these the reported cement content was the sum of cement and fly ash. One study used a geopolymer binder; one used dust collected by the foundry exhaust system rather than spent moulding sand, with a reported cement content that is inconsistent with its mix ratio; and one designed a separate mix for each fine aggregate. In one further study, WFS replaced slag sand in the control and WFS mixes alike; its five records were kept for the strength analyses but excluded from the index, because the avoided natural-sand credit does not apply. Every retained study that states or shows its replacement basis replaced sand by mass. The retained set comprises 196 records from 33 studies. Specimen type and cement type were not used as exclusion criteria, because each study used one specimen type and one cement for its control and WFS mixes; their effects were tested as sensitivities (Sections 4.5 and 4.9).

A units-consistency screen was applied. One source study (study 15 in Table S14) reported batch masses rather than per-cubic-meter quantities (its mix-design table lists cement as 44.1 kg/m^3 with 0.66 to 6.63 kg of WFS at 5% to 50% replacement, quantities that sum to about 212 kg; the database gives 3.63 kg for the 50% mix). For all records with

cement content below 150 kg/m^3 (six records, one study), the absolute-mass variables were set to missing, while the unit-free quantities (w/c, WFS %, strengths) were retained. After the screen, the observed ranges were w/c 0.40 to 0.56, WFS replacement 0% to 100% (median 20%), f'_c 19.0 to 56.0 MPa, elastic modulus 21.4 to 47.0 GPa, and cement content 300 to 479 kg/m^3 (Figure 12). The composite index could be computed for 173 mixes from 29 studies with complete mass information; the six screened records and 12 records from two other studies lacked cement or WFS mass, and the five slag-sand records were not indexed.

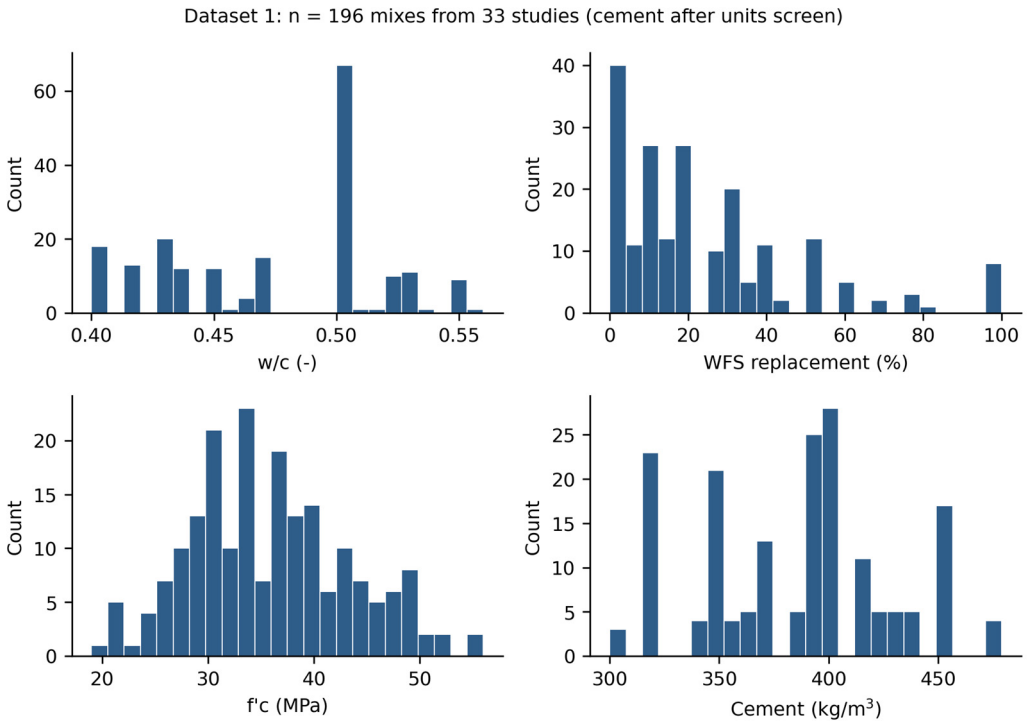


Figure 12. Distributions of w/c, WFS replacement, compressive strength, and cement content in the 196 retained records of the primary dataset (cement shown after the units screen).

4.2. Second Dataset

A second compilation of 430 WFS concrete records with full mix proportions (cement, silica fume, fly ash, water, natural sand, WFS, coarse and recycled coarse aggregates, superplasticizer, age, and compressive strength) was published by Hoang and Nguyen [21]. Restricting it to 28-day results with valid water and fine-aggregate entries and strengths below 100 MPa leaves 133 records. Twenty records containing recycled concrete aggregates were removed because they confounded the WFS effect, and one exact duplicate was removed, leaving 112 records; 24 of them contained silica fume or fly ash. Because the cost proxy prices cement as the only binder, the binder cost of these 24 records is understated, and they are excluded in a sensitivity check; in a bounding case, their silica fume and fly ash are priced at the cement price. As both compilations draw on the published WFS literature, the overlap between them was identified directly. Records of the second dataset were matched to the first when the cement content (within ±1 kg/m^3), w/c (within ±0.01), and WFS replacement (within ±1 percentage point) agreed. Furthermore, a mix series comprising records sharing cement, coarse aggregate, and superplasticizer contents was classified as overlapping whenever any member matched. Applying this rule identified 13 of 30 series and 68 of 112 records as probable overlaps, with matching mixes originating from 17 of the 40 primary source studies. Because matching on mix descriptors does not prove that two records are the same, the rule was repeated with stricter (±0.5 kg/m^3, ±0.005,

±0.5 percentage point) and looser (±5 kg/m^3, ±0.02, ±2.5 percentage points) tolerances, which gave 62 records in 11 overlapping series and 75 records in 17 (68 records in 13 series at baseline); the matches are therefore treated as probable overlap. The overlap flag of every record is given in Table S11a. Consequently, the second dataset cannot be considered independent, prompting Section 2.8 to report findings for both the full set and 44 non-overlapping records distributed across 17 series.

4.3. Auxiliary Benchmark Datasets

Two external datasets were used only as benchmarks and contained no WFS mixes. First, the compiled dataset of U.S. ready-mix concrete environmental product declarations (EPDs) by Broyles et al. [30] provides, for 38,944 declarations with a declared unit of 1 m^3 (39,213 records, of which 269 exact duplicates were removed), the A2 (transport to plant) contribution to global warming potential, which is used to verify the plausibility of the haul distance distributions. Second, the single-program laboratory database of Yeh [28] (1030 mixes with complete proportions and ages) served as a homogeneous control corpus for the surrogate-model test.

4.4. Framework Overview

Figure 1 summarizes this workflow. The source audit, data harmonization and quality control feed two assessment layers into the model. Layer 1 is a substitution decision index that asks whether and how much WFS to use within a mix family. Layer 2 is a cement-inclusive specification analysis that compares the competing mix designs. Each layer is supported by statistical, uncertainty, and diagnostic components, and the framework is re-applied to the second dataset as a consistency check.

4.5. Streamlined Carbon Accounting for Fine-Aggregate Substitution

The environmental criterion quantifies the net CO_2e effect of replacing natural sand with WFS at the mix level within the boundary of the concrete producer. Every retained study that states or shows its replacement basis replaced natural sand by mass (Table S14), so the baseline takes the displaced sand mass equal to the WFS mass, $m_{\mathrm{disp}} = m_{\mathrm{WFS}}$. A volumetric alternative, $m_{\mathrm{disp}} = m_{\mathrm{WFS}} \times (SG_{\mathrm{fa}}/SG_{\mathrm{WFS}})$, is kept as a sensitivity; it uses reported specific gravities where available (103 of the 196 retained records; ratio 0.94 to 1.26) and, in the uncertainty analysis, draws the ratio for the 55 WFS-bearing mixes without them from the observed ratios (missingness by study and replacement band in Table S15l). The net saving (kg CO_2e/m^3) is

$$\Delta CO_2 = \frac{1}{1000}\left[m_{\mathrm{disp}}\left(EF_{\mathrm{sand}} + EF_{\mathrm{tr}}\, d_{\mathrm{q}}\right) - m_{\mathrm{WFS}}\, EF_{\mathrm{tr}}\, d_{\mathrm{w}}\right] \quad (1)$$

where avoided sand production and quarry-to-plant haul scale with the displaced-sand mass, and the foundry-to-plant haul of WFS scales with the WFS mass. The baseline parameters were $EF_{\mathrm{sand}} = 5.5$ kg CO_2e/t, within the cradle-to-gate range reported for natural aggregates [35,36]; $EF_{\mathrm{tr}} = 0.12$ kg CO_2e/t·km, between the 2025 UK well-to-wheel factors for average-laden articulated (0.096) and rigid (0.241) diesel trucks [37]; $d_{\mathrm{q}} = 50$ km; and $d_{\mathrm{w}} = 30$ km. Because the avoided haul of WFS from the foundry to landfill and the avoided tipping fee accrue to the foundry, not to the concrete producer, both are excluded from the baseline. Instead, they are evaluated separately within a foundry-side scenario in which the landfill haul $d_{\mathrm{l}} = 50$ km and a tipping fee enter as credits. The volumetric alternative, applied to Equations (1) and (3) together, raises the median carbon credit by 16% but leaves the rankings essentially unchanged (Spearman rank correlation $\rho = 0.998$; top-quintile overlap 97%; ρ denotes Spearman's ρ throughout). Furthermore, batch-yield effects are

internalized directly at the study level, as each source publication reports quantities per cubic meter of produced concrete.

This is a streamlined, substitution-scope carbon account. Cement, water, admixtures, WFS beneficiation, plant energy, and all non-climate impact categories are outside its boundary (Table 3). At the dataset median cement content (390 kg/m^3), cement-attributable emissions are about 328 kg CO_2e/m^3 at EF_{cem} = 0.84 kg CO_2e/kg, the value reported for UK CEM I Portland cement [38], whereas the largest substitution saving in the dataset is 5.1 kg CO_2e/m^3 (8.9 kg CO_2e/m^3 under the foundry-side scenario). The binder is therefore handled in a separate specification layer, in which mixes compete on the cement-inclusive quantity

$$\mathrm{GWP} = EF_{cem}\, m_{cem} - \Delta CO_2 \quad (2)$$

with EF_{cem} varied between 0.58 kg CO_2e/kg, the 2023 global average for cement [39], and 0.84 kg CO_2e/kg. The baseline is deliberately set at the upper end of this range corresponding to CEM I Portland cement, ensuring conservative baseline GWP estimates. This factor is varied only in the Sobol analysis, and the Pareto set in Section 2.6 is identical at 0.58 and 0.84 kg CO_2e/kg. Eight retained studies used fly-ash-based Portland pozzolana cement and three used Portland-limestone cement (Table S14). Because each study used one cement for all its mixes, this does not affect the comparison of WFS mixes with their controls, but it lowers their cement factor. As a sensitivity, the factor for these studies was scaled by clinker share: 0.75 for Portland pozzolana cement, the midpoint of the 15% to 35% fly ash allowed by IS 1489 (Part 1) [40], and 0.87 for CEM II/A-L, the midpoint of the 6% to 20% limestone allowed by EN 197-1 [41]. Section 2.4 shows why this term cannot be embedded inside the weighted index.

Table 3. Scope of the environmental terms compared with a full cradle-to-gate life-cycle assessment (LCA).

Inventory Item	Full LCA	Index Term (Baseline)	Specification Layer
Natural sand production	Included	Included (mass basis)	Included
Quarry-to-plant and foundry-to-plant haul	Included	Included	Included
Foundry-to-landfill haul (avoided)	System-dependent	Foundry-side scenario only	Excluded
Cement production	Included	Excluded	Included
Water, admixtures, plant energy	Included	Excluded	Excluded
WFS beneficiation	Included	Excluded (break-even burden, Section 2.9)	Excluded
Non-climate impact categories	Included	Excluded	Excluded

Excluding WFS beneficiation favors WFS; therefore, the substitution saving is an upper estimate for sands that require processing. Section 2.9 gives the processing burden at which the saving is lost.

Because WFS beneficiation is outside the boundary, the processing burden at which the saving disappears was also computed. Per ton of WFS, Equation (1) on the mass basis gives a saving of $EF_{sand} + EF_{tr}(d_q - d_w)$; a processing step that emits more than this amount cancels the saving. As an example of such a step, thermal drying was estimated from an energy balance: heating the sand (specific heat 0.80 kJ/kg·K) and its moisture from 15 °C to 100 °C, evaporating the moisture (2257 kJ/kg), a dryer efficiency of 0.6 to 0.8, and natural gas at 56.1 kg CO_2/GJ [42]. Moisture contents of 2%, 5%, and 8% were evaluated.

4.6. Material-Cost Proxy

Because the primary dataset reports only the cement and WFS masses, the cost criterion is a proxy that captures the two components that vary across mixes, with the substitution differential computed on the same mass basis as Equation (1), in which the displaced sand

mass equals the WFS mass, and within the same boundary (the volumetric sensitivity in Section 4.5 changes Equations (1) and (3) together):

$$\text{Cost} = \frac{m_{\text{cem}}}{1000} P_{\text{cem}} - \frac{1}{1000}\left[m_{\text{disp}}\left(P_{\text{sand}} + c_{\text{tr}}\, d_{\text{q}}\right) - m_{\text{WFS}}\left(P_{\text{WFS}} + c_{\text{tr}}\, d_{\text{w}}\right)\right] \quad (3)$$

The baseline prices are P_{cem} = USD 155/t (USD 17 billion across an estimated 110 Mt of U.S. cement shipments in 2024 [43]), P_{sand} = USD 12.54/t (2023 average unit value of U.S. construction sand and gravel [43]), P_{WFS} = USD 2/t, reflecting that spent foundry sand is typically supplied at nominal cost [34,44], and a trucking cost c_{tr} = USD 0.07/t·km, derived from U.S. operational-trucking-cost data [45]. Cement dominates the approximation, approximately 78% of its variance across the 173 indexed mixes stems from cement content, resulting in cost correlating with cement content at $\rho = 0.96$ and with WFS mass at $\rho = -0.49$; therefore, the cost criterion functions mainly as a binder-cost axis. Within a family of mixes with the same cement content, however, the substitution differential in Equation (3) and the saving in Equation (1) both vary linearly with WFS mass, so E and K carry the same information there; Section 2.3 examines this with a variant in which K is the cement cost alone. In the foundry-side scenario, an avoided tipping fee (triangular USD 35, 62, 85/t; national average USD 62/t in 2024 [46]) is credited per ton of WFS. All prices entered the uncertainty analysis as distributions (Table 4).

Table 4. Parameter distributions and sources.

Parameter	Unit	Baseline	Distribution	Source
Natural sand production EF	kg CO_2e/t	5.5	Triangular (4.0, 5.5, 7.7)	[35,36]
Road freight EF (well-to-wheel)	kg CO_2e/t·km	0.12	Triangular (0.096, 0.12, 0.241)	[37]
Haul distances d_q, d_w (per mix)	km	50, 30	Uniform (10, 100)	Regional scenario
Landfill haul d_l (foundry-side only)	km	50	Uniform (10, 100)	Regional scenario
Cement EF (specification layer)	kg CO_2e/kg	0.84	Uniform (0.58, 0.84)	[38,39]
Cement price	USD/t	155	Triangular (120, 155, 180)	[43]
Sand price	USD/t	12.54	Triangular (8, 12.54, 16)	[43]
WFS price	USD/t	2	Triangular (0, 2, 10)	[34,44]
Trucking cost	USD/t·km	0.07	Triangular (0.05, 0.07, 0.12)	[45]
Tipping fee (foundry-side only)	USD/t	62	Triangular (35, 62, 85)	[46]

Note: EF, emission factor. The triangular distributions are given as (minimum, mode, and maximum).

4.7. Sub-Indices and Composite Index

The index uses three sub-indices on [0, 1], min–max normalized over the analyzed dataset, with higher values being preferred. The mechanical sub-index is $M = 0.60\, n(f'_c) + 0.25\, n(f_{st}) + 0.15\, n(E_c)$, with weights renormalized over the properties available for each record. For the 72 records with all three properties, the first principal component explained 76% of their variance and was correlated with M at Spearman $\rho = 0.99$. The environmental sub-index E is the normalized ΔCO_2 from Equation (1), and the cost sub-index K is the normalized negative cost from Equation (3). The composite is SI = wMM + wEE + wKK (per-mix values, Table S4). Because only 67 indexed mixes report all three properties, the index was also computed with M from compressive strength alone, for all mixes and for that complete-data subset. The records that set each normalization bound are listed in Table S15a; winsorized bounds (5th to 95th percentile), fixed reference bounds (f'_c 10 to 60 MPa, f_{st} 1 to 6 MPa, E_c 20 to 50 GPa, WFS 0 to 700 kg/m^3, cement 200 to 600 kg/m^3) and normalization over Datasets 1 and 2 pooled were tested as alternatives.

Two candidate metrics were intentionally omitted from the composite index and tracked as auxiliary indicators. Specifically, the circularity term, represented by the WFS replacement fraction, duplicates the information already captured by the environmental sub-index

(E), generating unacceptable variance inflation factors of 37.0 and 33.7 when co-included. Similarly, the cement-inclusive GWP cannot substitute for E because it and the cost criterion are heavily governed by cement content. Because min–max normalization scales values relative to the dataset itself, the resulting substitution index (*SI*) provides a comparative corpus-internal ranking rather than an absolute sustainability score.

4.8. Weighting and Aggregation

The baseline weights w_M, w_E, w_K were taken as 0.40, 0.35, 0.25 respectively to model a stakeholder scenario prioritizing mechanical adequacy. Three additional schemes were evaluated for comparison, including equal weights, entropy weights [47], and CRITIC weights [23]. To test sensitivity to the aggregation, mixes were ranked via TOPSIS [48], a distance-to-ideal method paired with CRITIC weights, providing an alternative to the weighted sum. Pairwise Spearman correlations and top-quintile overlap metrics summarize agreement across the five resulting ranking structures, while potential redundancy was evaluated using Spearman correlation matrices and variance inflation factors. A Derringer–Suich desirability index [49], calculated as the geometric mean of M, E, and K, served as a less compensatory cross-check. Because E = 0 for control mixes, the geometric mean assigns them a zero score by construction, necessitating that its correlation with *SI* be reported both overall and across the 138 WFS-bearing mixes.

Two sensitivity variants of the index were further constructed. A mechanical eligibility screen restricts evaluation to control mixes and those achieving a within-study relative strength of at least 0.95, ensuring that strength deficits are not offset by environmental or cost advantages. Because all 138 indexed WFS mixes report relative strength values, none were excluded for missing data. Finally, the foundry-side scenario incorporates avoided landfill hauls and tipping fees into *E* and *K*.

4.9. Statistical Analysis of the Dose-Response

The mechanical effect of WFS was estimated using a linear mixed-effects model with study random intercepts, $f'_c \sim x + x^2 + w/c + \text{cement}$, fitted by restricted maximum likelihood, where x = WFS replacement (%)/10, so that one unit of x is 10 percentage points; cement enters per 100 kg/m^3. This respects the data hierarchy, whereas pooled tests that ignore study clustering overstate significance. The within-study relative strength reported in the source database (strength divided by that of the same series at 0% WFS) is summarized by replacement band with medians and cluster-bootstrap 95% intervals (1000 resamples of whole studies). The same cluster bootstrap was used for median SI by band, and the Kruskal–Wallis test across bands is reported both on individual records and on study-level band medians. Because band medians from the same study remain dependent, a mixed model of SI on band with study random intercepts (likelihood-ratio test) and a within-study permutation test of the SI-replacement correlation (2000 permutations) were added.

Because the effect of WFS may differ between foundry sands, the model was refitted with a random slope on x by study, compared with the random-intercept model by a likelihood-ratio test (mixture of χ^2 distributions with 1 and 2 degrees of freedom), and used to give a 95% prediction interval for a new study; each study was also left out in turn. Equivalence with the control was tested with two one-sided tests at a margin of ±5% of the median control strength (±1.8 MPa): the change is equivalent when its 90% confidence interval lies within the margin. Because SI uses raw strengths, whereas the model absorbs study-level offsets, cube strengths were also converted to cylinder-equivalent values with a factor of 0.8, the cylinder-to-cube ratio of the EN 206 strength classes [50], and specimen type was added to the model as a covariate.

4.10. Uncertainty Propagation and Global Sensitivity

All uncertain parameters were assigned distributions anchored to the published sources (Table 4). Haul distances were sampled independently for each mix and leg, which allowed rankings to respond to logistics; a single global distance applied to all mixes would rescale ΔCO_2 almost uniformly and, after min–max normalization, would change rankings only through the mix-to-mix variation in the specific-gravity ratio. Because mixes from one study usually share suppliers, further distance schemes were run (1000 draws each): distances shared by all mixes of a study; shared within a study and correlated between the two legs (Gaussian copula, $\rho = 0.8$); and a single regional distance per draw. To separate parameter uncertainty from between-site variability, the parameters were also drawn with distances fixed, and the distances with parameters fixed, and a volumetric run drew the missing specific-gravity ratios for each study from the observed ratios. Monte Carlo propagation used 2000 draws; within each draw, the sub-indices were renormalized and the composite was recomputed. The reported outputs are per-mix medians and 95% intervals, the distribution of rank correlations between draws and the baseline, the rate at which mixes change SI quartiles, and the share of draws in which each mix is in the top quintile. Mixes in the top quintile in at least 90% of the draws form a robust short-list. First-order (S1) and total (ST) Sobol indices [51] were computed with Saltelli sampling [52] (2048 base samples) for ΔCO_2 and cement-inclusive GWP, evaluated for a representative mix at the median WFS (114 kg/m^3) and cement (390 kg/m^3) content.

4.11. Specification Layer: Non-Dominated Sorting and Function-Normalized Indices

The decision set comprises the collection of observed mixes. The primary specification analysis involves nondominated sorting within a three-objective space, aiming to maximize f′c, minimize cement-inclusive Global-Warming Potential (GWP), and minimize cost. This analysis is precise over the discrete set of observed designs, and non-dominance holds only within that set. Because GWP and cost are both governed by cement content, their pairwise correlations are reported, and the Pareto set was recomputed with substitution-scope carbon in place of GWP, at alternative cement and sand prices, with water added at an upper-bound factor of 0.001 kg CO_2e/kg, with the cement-type factors of Section 4.5, with cylinder-equivalent strengths, within subsets meeting minimum strengths of 25, 30 and 40 MPa, and in 500 Monte Carlo draws of all parameters. A continuous optimization over the design space, for example, with an evolutionary algorithm [53], would require a strength surrogate that is valid across the entire design space. Whether such a surrogate is defensible was tested using gradient-boosting regression under random five-fold and study-grouped five-fold cross-validation, first with mix descriptors (w/c, WFS %, cement) and then with the WFS characterization available in the database (fineness modulus, specific gravity, absorption, and WFS/cement ratio). As a control, the same model class was fitted to the Yeh database [28] with random five-fold cross-validation, using w/c, cement, and fine aggregate for the 28-day subset and all eight inputs for the full set. The Yeh data carry no study identifier; therefore, only random cross-validation is possible.

Per-cubic-meter indicators carry a known bias because strength determines the required member size. Consequently, a mix with a higher GWP per cubic meter can still produce a structural element with lower total GWP [3,32]. Following Kourehpaz and Miller [33] and Tavares et al. [31], two function-normalized index pairs were computed. For axially loaded short columns, where the required cross-section scales with $1/f'_c$, the eco- and cost-efficiency indices are $\chi_{col} = GWP/f'_c$ and $\kappa_{col} = cost/f'_c$. For beams sized against flexural cracking, depth scales with $f_r^{-0.5}$; with the strength relation used by Tavares et al. [31], $f_r = 0.75 {f'_c}^{0.5}/\lambda^2$ with $\lambda = 1.1125 \exp(-0.004 f'_c)$, the indices become $\chi_{crk} = \lambda\ GWP/{f'_c}^{0.25}$ and $\kappa_{crk} = \lambda\ Cost/{f'_c}^{0.25}$. Lower is better in all four, and non-dominated sorting is applied in

each (χ, κ) plane. The association between χ_{col} and WFS content was assessed pooled, with a study-cluster bootstrap interval, and within studies, with a within-study permutation test.

4.12. Cross-Compilation Consistency Protocol

The framework was re-applied to the second dataset with the same structure, weights, parameters, and boundary. Because only the compressive strength was available, M was reduced to normalized f'_c, and ΔCO_2 used the mass basis. For a like-for-like comparison, Dataset 1 was also indexed with M from compressive strength alone. Intervals for the Dataset 2 correlations and entropy weights were obtained by resampling mix series (1000 resamples), because records within a series share materials. The reported metrics are the rank agreement among the five methods, SI-WFS association, median strength by replacement band, entropy weight on E, and VIF range of the three criteria for the fully cleaned set and non-overlapping subset. This exercise evaluates whether the qualitative characteristics of the framework are applicable to a different compilation. However, it does not demonstrate that SI measures sustainability, as this would necessitate external criteria, such as expert elicitation or procurement outcomes.

4.13. Software and Reproducibility

All analyses were run in Python 3.13 (NumPy 2.4.4, pandas 3.0.2, SciPy 1.17.1, statsmodels 0.15.0, scikit-learn 1.8.0, SALib 1.6.0, and matplotlib 3.10.9) with a fixed random seed, and the code, the source audit and all derived tables are provided in the Supplementary Materials.

5. Conclusions

A two-layer assessment framework for WFS concrete was developed and tested on two literature compilations after a source-by-source audit of the primary data. Six conclusions follow. First, once between-study heterogeneity is modeled, 28-day compressive strength is equivalent to the control within $\pm$1.8 MPa up to 30% replacement ($-$0.5 MPa at 30%, 95% CI $-$2.0 to 1.0), shows no detectable average loss at 50% ($-$1.7 MPa, CI $-$3.6 to 0.2), and falls clearly only at high replacement ($-$8.0 MPa at 100%); this applies to 28-day strength only. The effect varies between foundry sands (95% prediction interval $-$10 to +9 MPa at 30%), so each new source must be tested. Second, the three criteria show limited collinearity across the corpus (VIF 1.03 to 1.50) and the rankings are robust to weighting, aggregation, and normalization ($\rho \geq 0.84$); within a mix family, the carbon and cost criteria carry the same substitution signal, which a cement-only cost variant removes without changing the rankings. A mechanically screened variant is available where strength penalties are unacceptable. Third, the cement-inclusive term is redundant inside a weighted sum (VIF about 24) but essential for specification, where, among the observed mixes and under the baseline scenario, none with more than 355 kg/m^3 of cement is Pareto-efficient; function-normalized indices favor the strongest mixes in the column case, and WFS content is not associated with improving them. Fourth, haul-distance uncertainty dominates the substitution layer: thirteen mixes remain in the top quintile in at least 90% of draws, and nine of them under every distance scheme tested. Logistics decide whether the small substitution saving materializes, and the binder decides the climate performance of the concrete. Fifth, the substitution saving is at most 5.1 kg CO_2e/m^3 and is lost if processing emits more than about 8 kg CO_2e per ton of WFS at baseline haul distances, a burden that the estimated emissions of kiln drying would exceed. Sixth, a strength surrogate trained on pooled literature data does not generalize across studies (grouped $R^2 = -0.74$, and $-$0.44 with the available WFS characterization), which identifies standardized WFS characterization (clay content, loss on ignition, binder type) as the reporting gap that blocks

transferable strength models. The code, source audit, parameter distributions, and derived tables are provided so that the framework can be re-parameterized for other regions and extended to durability when data allow.

Supplementary Materials: The following supporting information can be downloaded at: https://www.mdpi.com/article/10.3390/recycling11120210/s1, Table S1: Primary dataset (233 compiled mixes, 40 studies) with study identifiers, quality-control flags and inclusion status after the source audit; Table S2: Spearman correlations among the index criteria (M, E, K) and the auxiliary indicators (n = 173 indexed mixes); Table S3a: Criterion weights by weighting method (primary dataset); Table S3b: Spearman rank agreement among the five ranking methods (n = 173); Table S3c: Share of the top quintile (35 mixes) shared by each pair of ranking methods; Table S4: Per-mix results for the 173 indexed mixes; Table S5a: Mixed-effects model for 28-day compressive strength with study random intercepts (n = 178 mixes, 30 studies); Table S5b: Covariate-adjusted 28-day strengths plotted in Figure 3a (n = 178); Table S5c: Within-study relative strength (f′c/f′c at 0% WFS) by replacement band, with cluster-bootstrap 95% intervals (156 records, 33 studies); Table S5d: Mixed-effects model without the 28 retained records flagged as outliers in the source database (n = 150); Table S6: Monte Carlo results per mix (2000 draws): SI median and 95% interval, and share of draws in the top quintile; Table S7a: First-order (S1) and total (ST) Sobol indices for the substitution-scope carbon saving (ΔCO_2); Table S7b: First-order (S1) and total (ST) Sobol indices for the cement-inclusive GWP; Table S8: Pareto-efficient mixes in the specification space (maximum f′c, minimum cement-inclusive GWP, minimum cost); Table S9: Function-normalized eco-efficiency (χ) and cost-efficiency (κ) indices for the column and cracking cases; Table S10: Median SI by WFS replacement band with cluster-bootstrap 95% intervals (n = 173); Table S11a: Second dataset [21]: 112 cleaned 28-day records, overlap with the primary dataset and results; Table S11b: Median 28-day compressive strength (MPa) by WFS replacement band; Table S11c: Spearman rank agreement among the five ranking methods in the second dataset (n = 112); Table S11d: Second dataset: sensitivity subsets; Table S12: Index sensitivities per mix: baseline SI and SI under the mechanical eligibility screen, the foundry-side scenario and exclusion of flagged outliers; Table S13: A2 (transport to plant) and A1–A3 GWP of 38,944 U.S. ready-mix concrete EPDs [30], summary statistics; Table S14: Source audit of the 40 primary studies of Iqbal et al. [14]: replacement basis, specimen used for 28-day compressive strength, cement, and inclusion decision; Table S15a: Records that set the minimum and maximum of each min-max normalized variable (173 indexed mixes); Table S15b: Index under alternative normalizations, compared with the baseline min-max normalization; Table S15c: Index with the mechanical criterion from compressive strength alone; Table S15d: Monte Carlo results under alternative haul-distance dependence and with uncertainty sources separated (1000 draws per scenario); Table S15e: Pareto set (maximum f′c, minimum GWP, minimum cost) under alternative objectives, prices, thresholds and Monte Carlo draws; Table S15f: Mixed-effects WFS effect with each study left out in turn; Table S15g: Equivalence of the WFS strength effect with the control (two one-sided tests; margin ± 5% of the median control strength, ± 1.83 MPa); Table S15h: Second dataset: intervals from resampling mix series (1000 resamples) and bound for the unpriced silica fume and fly ash; Table S15i: Thermal drying of WFS compared with the break-even processing burden (7.9 kg CO_2e per tonne of WFS at baseline); Table S15j: Index results under a uniform WFS processing burden; Table S15k: Per-mix outputs of the revision analyses: cylinder-equivalent strength, SI with cement-only cost, share of Monte Carlo draws on the Pareto set, and share of draws in the top quintile under each distance scenario; Table S15l: Missing specific-gravity ratios among the 156 retained WFS-bearing mixes (used only in the volumetric sensitivity); analysis and figure scripts.

Author Contributions: Conceptualization, F.N.; methodology, F.N.; software, F.N.; formal analysis, F.N.; data curation, F.N.; writing—original draft preparation, F.N.; writing—review and editing, F.N. and A.O.; visualization, F.N.; supervision, A.O. All authors have read and agreed to the published version of the manuscript.

Funding: This research received no external funding. The APC was funded by the University of Johannesburg.

Data Availability Statement: The data analyzed in this study came from the primary dataset of Iqbal et al. [14], the second dataset of Hoang and Nguyen [21], the EPD dataset of Broyles et al. [30], and the concrete data of Yeh [28] (UCI Machine Learning Repository). The original contributions presented in this study are included in the article and Supplementary Material. Further inquiries can be directed to the corresponding author.

Acknowledgments: Authors thank the University of Johannesburg for providing an enabling research environment and support.

Conflicts of Interest: The authors declare no conflicts of interest.

Abbreviations

Abbreviations used in this manuscript are as follows:

A1–A3	EPD modules for raw material supply (A1), transport to plant (A2) and manufacturing (A3)
CI	Confidence interval
CRITIC	Criteria Importance Through Intercriteria Correlation
EF	Emission factor
EPD	Environmental product declaration
GWP	Global warming potential
LCA	Life-cycle assessment
PCA	Principal component analysis
SCM	Supplementary cementitious material
SI	Substitution index (composite)
TOPSIS	Technique for Order of Preference by Similarity to Ideal Solution
VIF	Variance inflation factor
WFS	Waste foundry sand

References

1. United Nations Environment Programme. *Sand and Sustainability: 10 Strategic Recommendations to Avert a Crisis*; GRID-Geneva, UNEP: Geneva, Switzerland, 2022. Available online: https://www.unep.org/resources/report/sand-and-sustainability-10-strategic-recommendations-avert-crisis (accessed on 25 September 2026).
2. Flower, D.J.M.; Sanjayan, J.G. Greenhouse Gas Emissions Due to Concrete Manufacture. In *Handbook of Low Carbon Concrete*; Nazari, A., Sanjayan, J.G., Eds.; Butterworth-Heinemann: Oxford, UK, 2017; pp. 1–16. [CrossRef]
3. Miller, S.A.; Horvath, A.; Monteiro, P.J.M. Readily Implementable Techniques Can Cut Annual CO2 Emissions from the Production of Concrete by over 20%. *Environ. Res. Lett.* **2016**, *11*, 074029. [CrossRef]
4. Niu, D.; Zhou, J.; Guo, B. Carbon Footprint Dataset of Concrete Based on Field Surveys at Commercial Mixing Plants in Shandong, China. *Sci. Data* **2026**, *13*, 465. [CrossRef]
5. Marsh, A.T.M.; Velenturf, A.P.M.; Bernal, S.A. Circular Economy Strategies for Concrete: Implementation and Integration. *J. Clean. Prod.* **2022**, *362*, 132486. [CrossRef]
6. Chesner, W.H.; Collins, R.J.; MacKay, M.H. *User Guidelines for Waste and Byproduct Materials in Pavement Construction*; FHWA-RD-97-148; Federal Highway Administration: McLean, VA, USA, 1998. Available online: https://www.fhwa.dot.gov/publications/research/infrastructure/pavements/97148/027.cfm (accessed on 25 September 2026).
7. U.S. Environmental Protection Agency. Beneficial Uses of Spent Foundry Sands. Available online: https://www.epa.gov/smm/beneficial-uses-spent-foundry-sands (accessed on 25 September 2026).
8. Siddique, R.; Singh, G. Utilization of Waste Foundry Sand (WFS) in Concrete Manufacturing. *Resour. Conserv. Recycl.* **2011**, *55*, 885–892. [CrossRef]
9. Singh, G.; Siddique, R. Effect of Waste Foundry Sand (WFS) as Partial Replacement of Sand on the Strength, Ultrasonic Pulse Velocity and Permeability of Concrete. *Constr. Build. Mater.* **2012**, *26*, 416–422. [CrossRef]
10. Kaur, G.; Siddique, R.; Rajor, A. Properties of Concrete Containing Fungal Treated Waste Foundry Sand. *Constr. Build. Mater.* **2012**, *29*, 82–87. [CrossRef]
11. Iloh, P.; Fanourakis, G.; Ogra, A. Evaluation of Physical and Chemical Properties of South African Waste Foundry Sand (WFS) for Concrete Use. *Sustainability* **2019**, *11*, 193. [CrossRef]
12. Sandhu, R.K.; Siddique, R. Strength Properties and Microstructural Analysis of Self-Compacting Concrete Incorporating Waste Foundry Sand. *Constr. Build. Mater.* **2019**, *225*, 371–383. [CrossRef]

13. García, G.; Cabrera, R.; Rolón, J.; Pichardo, R.; Thomas, C. Systematic Review on the Use of Waste Foundry Sand as a Partial Replacement of Natural Sand in Concrete. *Constr. Build. Mater.* **2024**, *430*, 136460. [CrossRef]
14. Iqbal, M.F.; Liu, Q.-f.; Azim, I.; Zhu, X.; Yang, J.; Javed, M.F.; Rauf, M. Prediction of Mechanical Properties of Green Concrete Incorporating Waste Foundry Sand Based on Gene Expression Programming. *J. Hazard. Mater.* **2020**, *384*, 121322. [CrossRef]
15. Behnood, A.; Golafshani, E.M. Machine Learning Study of the Mechanical Properties of Concretes Containing Waste Foundry Sand. *Constr. Build. Mater.* **2020**, *243*, 118152. [CrossRef]
16. Tavana Amlashi, A.; Alidoust, P.; Pazhouhi, M.; Pourrostami Niavol, K.; Khabiri, S.; Ghanizadeh, A.R. AI-Based Formulation for Mechanical and Workability Properties of Eco-Friendly Concrete Made by Waste Foundry Sand. *J. Mater. Civ. Eng.* **2021**, *33*, 04021038. [CrossRef]
17. Iqbal, M.F.; Javed, M.F.; Rauf, M.; Azim, I.; Ashraf, M.; Yang, J.; Liu, Q.-f. Sustainable Utilization of Foundry Waste: Forecasting Mechanical Properties of Foundry Sand Based Concrete Using Multi-Expression Programming. *Sci. Total Environ.* **2021**, *780*, 146524. [CrossRef]
18. Mehta, V. Machine Learning Approach for Predicting Concrete Compressive, Splitting Tensile, and Flexural Strength with Waste Foundry Sand. *J. Build. Eng.* **2023**, *70*, 106363. [CrossRef]
19. Javed, M.F.; Khan, M.; Fawad, M.; Alabduljabbar, H.; Najeh, T.; Gamil, Y. Comparative Analysis of Various Machine Learning Algorithms to Predict Strength Properties of Sustainable Green Concrete Containing Waste Foundry Sand. *Sci. Rep.* **2024**, *14*, 14617. [CrossRef]
20. Alizamir, M.; Wang, M.; Ikram, R.M.A.; Gholampour, A.; Ahmed, K.O.; Heddam, S.; Kim, S. An Interpretable XGBoost-SHAP Machine Learning Model for Reliable Prediction of Mechanical Properties in Waste Foundry Sand-Based Eco-Friendly Concrete. *Results Eng.* **2025**, *25*, 104307. [CrossRef]
21. Hoang, N.-D.; Nguyen, Q.-L. Toward Sustainable Construction: Estimating Compressive Strength of Waste Foundry Sand-Blended Green Concrete Using a Hybrid Machine Learning Approach. *Discov. Civ. Eng.* **2025**, *2*, 42. [CrossRef]
22. Saaty, R.W. The Analytic Hierarchy Process—What It Is and How It Is Used. *Math. Model.* **1987**, *9*, 161–176. [CrossRef]
23. Diakoulaki, D.; Mavrotas, G.; Papayannakis, L. Determining Objective Weights in Multiple Criteria Problems: The CRITIC Method. *Comput. Oper. Res.* **1995**, *22*, 763–770. [CrossRef]
24. Nardo, M.; Saisana, M.; Saltelli, A.; Tarantola, S. *Tools for Composite Indicators Building*; EUR 21682 EN; European Commission, Joint Research Centre: Ispra, Italy, 2005. Available online: https://knowledge4policy.ec.europa.eu/sites/default/files/eur_21682_en_1.pdf (accessed on 25 September 2026).
25. OECD; European Union; Joint Research Centre. *Handbook on Constructing Composite Indicators: Methodology and User Guide*; OECD Publishing: Paris, France, 2008. [CrossRef]
26. Miller, S.A.; Moore, F.C. Climate and Health Damages from Global Concrete Production. *Nat. Clim. Change* **2020**, *10*, 439–443. [CrossRef]
27. Kurda, R.; de Brito, J.; Silvestre, J.D. CONCRETop—A Multi-Criteria Decision Method for Concrete Optimization. *Environ. Impact Assess. Rev.* **2019**, *74*, 73–85. [CrossRef]
28. Yeh, I.-C. Modeling of Strength of High-Performance Concrete Using Artificial Neural Networks. *Cem. Concr. Res.* **1998**, *28*, 1797–1808. [CrossRef]
29. Ganesh Prabhu, G.; Hyun, J.H.; Kim, Y.Y. Effects of Foundry Sand as a Fine Aggregate in Concrete Production. *Constr. Build. Mater.* **2014**, *70*, 514–521. [CrossRef]
30. Broyles, J.M.; Gevaudan, J.P.; Brown, N.C. A Compiled Dataset of Ready-Mix Concrete Environmental Product Declarations for Life Cycle Assessment. *Data Brief* **2024**, *52*, 109852. [CrossRef]
31. Tavares, C.; Skillen, K.; Shi, X.; Grasley, Z. Multi-Criteria Comparison Tools to Evaluate Cost- and Eco-Efficiency of Ultra-High-Performance Concrete. *Environ. Res. Infrastruct. Sustain.* **2023**, *3*, 025010. [CrossRef]
32. Damineli, B.L.; Kemeid, F.M.; Aguiar, P.S.; John, V.M. Measuring the Eco-Efficiency of Cement Use. *Cem. Concr. Compos.* **2010**, *32*, 555–562. [CrossRef]
33. Kourehpaz, P.; Miller, S.A. Eco-Efficient Design Indices for Reinforced Concrete Members. *Mater. Struct.* **2019**, *52*, 96. [CrossRef]
34. U.S. Environmental Protection Agency. *Risk Assessment of Spent Foundry Sands in Soil-Related Applications: Evaluating Silica-Based Spent Foundry Sand from Iron, Steel, and Aluminum Foundries*; EPA-530-R-14-003; U.S. EPA Office of Resource Conservation and Recovery: Washington, DC, USA, 2014. Available online: https://www.epa.gov/sites/default/files/2016-03/documents/risk_assessment_sfs_in_soil.pdf (accessed on 25 September 2026).
35. de Bortoli, A. Understanding the Environmental Impacts of Virgin Aggregates: Critical Literature Review and Primary Comprehensive Life Cycle Assessments. *J. Clean. Prod.* **2023**, *415*, 137629. [CrossRef]
36. Li, N.; Zhang, Z.; Hu, D.; Pang, G.; Wang, Q.; Si, W. Economic and Carbon Emission Analyses of C50 Manufactured Sand Concrete Considering Workability and Compressive Strength. *Buildings* **2025**, *15*, 77. [CrossRef]

37. Department for Energy Security and Net Zero. *Greenhouse Gas Reporting: Conversion Factors 2025*; DESNZ: London, UK, 2025. Available online: https://www.gov.uk/government/publications/greenhouse-gas-reporting-conversion-factors-2025 (accessed on 25 September 2026).
38. Mineral Products Association. *Fact Sheet 18: Embodied CO2e of UK Cements, Additions and Cementitious Material, Revision 4*; MPA: London, UK, 2025. Available online: https://cement.mineralproducts.org/MPACement/media/Cement/Publications/Fact-Sheets/FS_18_Embodied_CO2e.pdf (accessed on 25 September 2026).
39. World Economic Forum. *Net-Zero Industry Tracker 2024: Cement*; WEF: Geneva, Switzerland, 2024. Available online: https://reports.weforum.org/docs/WEF_Net_Zero_Industry_Tracker_2024_Cement.pdf (accessed on 25 September 2026).
40. *IS 1489 (Part 1): 2015*; Portland Pozzolana Cement—Specification, Part 1: Fly Ash Based. BIS: New Delhi, India, 2015.
41. *EN 197-1:2011*; Cement—Part 1: Composition, Specifications and Conformity Criteria for Common Cements. CEN: Brussels, Belgium, 2011.
42. Intergovernmental Panel on Climate Change. *2006 IPCC Guidelines for National Greenhouse Gas Inventories, Volume 2: Energy, Chapter 2: Stationary Combustion*; IGES: Hayama, Japan, 2006. Available online: https://www.ipcc-nggip.iges.or.jp/public/2006gl/vol2.html (accessed on 7 November 2026).
43. U.S. Geological Survey. *Mineral Commodity Summaries 2025*; USGS: Reston, VA, USA, 2025. [CrossRef]
44. Benson, C.H.; Bradshaw, S. *User Guideline for Foundry Sand in Green Infrastructure Construction*; Recycled Materials Resource Center, University of Wisconsin–Madison: Madison, WI, USA, 2011. Available online: https://rmrc.wisc.edu/wp-content/uploads/2012/11/Bradshaw-No.-59-Part-4-Updated-Beneficial-User-Guidelines-Foundry-Sand2.pdf (accessed on 25 September 2026).
45. Leslie, A.; Murray, D. *An Analysis of the Operational Costs of Trucking: 2024 Update*; American Transportation Research Institute: Arlington, VA, USA, 2024. Available online: https://truckingresearch.org/2024/06/an-analysis-of-the-operational-costs-of-trucking-2024-update/ (accessed on 25 September 2026).
46. Environmental Research & Education Foundation. *2024 Analysis of Municipal Solid Waste (MSW) Landfill Tipping Fees*; EREF: Raleigh, NC, USA, 2025. Available online: https://erefdn.org/product/2024-analysis-of-municipal-solid-waste-msw-landfill-tipping-fees/ (accessed on 25 September 2026).
47. Shannon, C.E. A Mathematical Theory of Communication. *Bell Syst. Tech. J.* **1948**, *27*, 379–423. [CrossRef]
48. Hwang, C.-L.; Yoon, K. *Multiple Attribute Decision Making: Methods and Applications*; Lecture Notes in Economics and Mathematical Systems; Springer: Berlin/Heidelberg, Germany, 1981. [CrossRef]
49. Derringer, G.; Suich, R. Simultaneous Optimization of Several Response Variables. *J. Qual. Technol.* **1980**, *12*, 214–219. [CrossRef]
50. *EN 206:2013+A2:2021*; Concrete—Specification, Performance, Production and Conformity. CEN: Brussels, Belgium, 2021.
51. Sobol', I.M. Global Sensitivity Indices for Nonlinear Mathematical Models and Their Monte Carlo Estimates. *Math. Comput. Simul.* **2001**, *55*, 271–280. [CrossRef]
52. Saltelli, A.; Ratto, M.; Andres, T.; Campolongo, F.; Cariboni, J.; Gatelli, D.; Saisana, M.; Tarantola, S. *Global Sensitivity Analysis: The Primer*; Wiley: Chichester, UK, 2008. [CrossRef]
53. Deb, K.; Pratap, A.; Agarwal, S.; Meyarivan, T. A Fast and Elitist Multi-objective Genetic Algorithm: NSGA-II. *IEEE Trans. Evol. Comput.* **2002**, *6*, 182–197. [CrossRef]

Disclaimer/Publisher's Note: The statements, opinions and data contained in all publications are solely those of the individual author(s) and contributor(s) and not of MDPI and/or the editor(s). MDPI and/or the editor(s) disclaim responsibility for any injury to people or property resulting from any ideas, methods, instructions or products referred to in the content.